Misan Journal of Engineering Sciences ISSN: 2957-4250
Vol. 5, No. 1, 28 June 2026 ISSN-E: 2957-4242

Numerical Analysis of the Effect of Porous Structure on Pressure Distribution in Heat Exchangers Using CFD

Muntadher H. Mohammed*[1],

[1] *Department of Mechanical Engineering, Islamic Azad University of Science and Research Branch, Tehran, Iran*

**Corresponding author E-mail: enginman3@gmail.com*

(Received 10 March, Revised 9 May, Accepted 9 May)

Abstract: This study aims to investigate the effect of the arrangement of porous layers on pressure drop through a numerical simulation using CFD techniques in ANSYS Fluent software. In this study, a two-dimensional model was constructed for a horizontal channel containing three consecutive porous layers with different values of porosity, such that they are arranged transversely within the channel. The simulations were carried out for six different porous layer arrangements, where only the positions of these layers were swapped with each other in these cases without changing the porous values or the thickness of layers. While keeping all parameters of the simulation unchanged, including the outlet pressure and the air inlet velocity. The results comparison showed that by changing the arrangement of the porous layers, the pressure losses can be reduced by up to 34.5% while maintaining a relatively high value of pressure at the outlet of these layers. This, in turn, improves the operational efficiency by choosing the arrangement that achieves the least resistance and therefore the least losses.

Keywords: Porosity, pressure drop, porous media, heat transfer, pressure losses.

1. Introduction

Achieving the optimal rate of heat transfer and the highest thermal efficiency of heat exchangers [1] is considered one of the most important design stages in various thermal systems. One of the most important factors affecting the performance of these systems is the properties of the medium through which the fluid flows [2].

The engineering analyses of fluid dynamics [3] indicate that the addition of porous layers inside the fluid flow channels in heat exchangers can improve the overall thermal efficiency of the heat exchanger [4].

However, this in turn leads to a pressure drop of the fluid as a result of its passage through the porous media, which affects the operating performance [5].

Porosity is considered one of the most important structural properties that directly affects flow behavior and heat transfer in thermal systems, as the presence of a porous medium in the heat exchanger increases the contact surface area between the fluid and the channel wall, which enhances heat transfer and improves the quality and performance of the thermal system [6].

Despite the advantages of these porous media, they lead to an increase in flow resistance [7], which causes a greater pressure drop of the fluid across these porous layers [8]. One of the most important factors affecting flow resistance, and consequently the pressure drop, is the porosity value, the geometric properties of the porous medium, and the arrangement of these layers within the heat exchangers [9].

Hence, this study illustrates the effect of consecutive porous layers with different porosity values on pressure variation and flow characteristics, and it also aims to investigate the impact of the arrangement of these layers on flow behavior. This is intended to achieve the optimal balance between heat transfer rate and the minimization of pressure losses in various thermal systems.

DOI: https://doi.org/10.61263/mjes.v5i1.282

This work is licensed under a Creative Commons Attribution 4.0 International License.

2. Previous Studies

Numerous previous studies have investigated the effect of pressure when fluids flow through porous materials in heat exchangers using CFD techniques. Among these studies:

Marcello. L et al. conducted a comparison between the real porous structure of metallic foam and the idealized Kelvin foam structure, in terms of pressure values and heat transfer rate, using CFD techniques in 2014, the result of this study showed differences in the heat transfer values, particularly at high Reynolds numbers, whereas the pressure values and their variations (pressure drop) were in close agreement, with a high degree of convergence approaching nearly 100% [10].

In another study conducted in the same year by Weiping W. et al., the relationship between flow distribution, Reynolds number and pressure drop were clarified, based on the analysis of flow distribution and pressure drop values at different Reynolds numbers [11].

Osama H. et al., in a study conducted in 2022, concluded that the pressure decreases further as the porosity decreases. This was demonstrated through a study of heat transfer and pressure drop for turbulent air flow in a porous channel [12].

In 2023, Gendera and Ludwing presented a CFD model for pressure drop in a double-pipe heat exchanger equipped with turbulators representing the porous medium. They were able to calculate the pressure losses, which were found to be close to the experimental values [13].

Lu et al. conducted a numerical study in 2024 on fluid flow through layers with different porosities. It was found that heat transfer, permeability, and pressure distribution values vary depending on the structural properties of the porous layer [14].

Also in 2024, Bahrami. H. R. & Sharifi. A. E. studied the effect of the arrangement of porous layers on heat transfer and pressure drop. They studied five cases of the arrangement of porous layers, but they focused on the longitudinal placement of the porous layers along the entire length of the channel and changing their arrangement from the pipe wall towards the center. They concluded that the arrangement of the porous layers directly affects the heat transfer coefficient and pressure drop, and thus the performance of the heat exchanger. This study indicated that pressure drop can be reduced by up to 20% [15].

In a more recent study in 2025, B. Jayrman and K. Mashesh used wire meshes to represent the porous medium to enhance the performance of heat exchangers [16].

Also in 2025, Hameed and Ali investigated a horizontal tubular heat exchanger composed of multiple layers of porous materials. Their study showed that while thermal efficiency is significantly enhanced, variation in the friction factor leads to increased pressure losses, resulting in a higher pressure drop [17].

These studies indicated that the use of porous media enhances the heat transfer efficiency in heat exchangers, thereby improving the overall thermal performance of the exchangers. However, at the same time, they lead to a pressure drop of the fluid flowing through these porous media. Few studies, however, have addressed the behavior of fluid flow through layers with different geometric properties and the effect of the arrangement of these layers on the flow characteristics or fluid behavior. Especially the effect of the arrangement of these layers on the pressure drop, such as the study by Bahrami and Sharifi, which focused on the longitudinal placement of the layers along the entire length of the channel.

Previous studies have shown considerable interest in analyzing flow within porous media using various numerical and experimental models. However, many of them have focused on simplified cases without adequately addressing the effect of the arrangement of porous layers. It is also observed that the treatment of the impact of the structural distribution of the porous medium remains limited in several of these studies, which opens the door for further research in this area.

Accordingly, this research focused on studying the effect of the arrangement of the porous layers on the pressure drop, where the porous layers are placed transversely. This is considered an important factor that directly affects the operating efficiency of heat exchangers and systems.

3. Research Methodology

This paragraph will review the mathematical models, sketch design in ANSYS Workbench, mesh, and parameters to adjust the numerical simulation setting.

3.1 Theoretical foundations

The presence of porous media in heat exchangers increases the heat transfer surface area and causes flow disturbance within the porous medium. This leads to an increase in the amount of heat transferred, but at the same time, the flow resistance increases.

To analyze the flow characteristics of fluids through porous media using Computational Fluid Dynamics (CFD) techniques in ANSYS Fluent, the basic equations that link pressure, flow properties, and the characteristics of the porous medium are relied upon [18].

The most important of these equations are [3,19,20]:

1- Reynolds number equation: This equation is used to determine the flow type within the channel.

$$Re = \frac{\rho u}{\mu} D \tag{1}$$

2- Darcy's Equation: This equation is used at low velocities, and thus for linear flow, to express the flow rate as a function of pressure and permeability.

$$u = -\frac{k}{\mu} \nabla P \tag{2}$$

3- Forchheimer Equation: This equation is considered an extension of Darcy's equation and is used to understand the effect of high velocities and turbulent flow in porous media.

$$-\nabla P = \frac{\mu}{k} u + \rho \beta u^2 \tag{3}$$

4- Brinkman Equation: This equation takes into account the effect of the internal viscosity of the fluids.

$$-\nabla P + \mu_{eff} \nabla^2 u = \frac{\mu}{k} u \tag{4}$$

5- Ergun Equation: Ergun's equation is used to calculate the pressure drop in porous layers as a function of viscosity, fluid density and flow speed. This equation is the sum of two terms; the first term represents the viscous resistance, while the second term represents the inertial resistance [21].

$$\frac{\nabla \mathrm{P}}{L} = \frac{150\mu(1-\varepsilon)^2}{d_p^2 \varepsilon^3} u + \frac{1.75\rho(1-\varepsilon)}{d_p \varepsilon^3} u^2 \tag{5}$$

Where:

β: Forchheimer coefficient, which represents the nonlinear resistance resulting from high velocity values.

μ_{eff}: effective fluid viscosity (which takes into account the effect of the porous media).

These equations form the theoretical basis for analyzing pressure losses and flow characteristics in porous media, and CFD techniques rely on them to obtain accurate results that are as close as possible to real-world outcomes, thereby reducing the effort and cost of difficult-to-perform experiments. These techniques enable optimizing the design using porous media to achieve the best thermal efficiency and the lowest pressure losses before the practical implementation of the design.

3.2 Numerical simulation methodology in ANSYS

This study was conducted using CFD simulation in ANSYS Fluent to investigate the effect of a multi-layer porous medium with different porosity values on the pressure drop in heat exchangers.

This simulation focused on comparing the effect of the arrangement of porous layers on pressure drop and

pressure distribution (pressure variation) along the channel, where a channel containing a porous medium with three layers of different porosity values was designed.
Since the number of porous layers is three, there are six cases for these layers to be placed within the channel that are considered in these simulations. These six arrangements are shown in table (7) which displays simulation results in each case.
The properties of the fluid (air) and the porous media were specified, including viscosity and porosity, as well as the initial temperature and flow velocity of the air.
Source term models were used within ANSYS to implement the Darcy, Brinkman, Forchheimer and Ergun equations and to study the pressure variation within the porous media.

Table 1 Porous layer properties.

Porosity ε	Permeability $k\ [m^2]$	Viscous resistance coefficient $1/k$ $[m^{-2}]$	Inertial resistance coefficient C_2 $[m^{-1}]$
0.7	2.12×10^{-10}	4.7×10^{9}	1.25×10^{4}
0.6	6.25×10^{-11}	1.6×10^{10}	3.24×10^{4}
0.5	2.78×10^{-11}	3.6×10^{10}	1.4×10^{5}

Table (1) shows the characteristics of the porous layers that were used in the study, including porosity, permeability, and coefficients of both viscous and inertial resistance.
For modeling the porous medium, the porous media model with the Darcy-Forchheimer formulation was used in ANSYS Fluent, since the flow occurs in a regime where both viscous and inertial effects are present. The viscous and inertial resistance coefficients were also calculated using the Ergun correlation.
The mesh: A structured quad mesh with a small element size was used to ensure the accuracy of the simulation, where an element size of $0.0001m$ was specified.
After generating the mesh, the number of elements was 17500, and the number of nodes was 17901. The mesh quality was then evaluated using the skewness and orthogonality criteria shown in table (2), where it was confirmed that the values were within acceptable limits before starting the numerical solution process.

Table 2 Mesh quality assessment.

	min	max	average	Standard deviation
Skewness	1.3057×10^{-10}	2.5107×10^{-2}	3.3548×10^{-4}	1.8099×10^{-3}
Orthogonality	0.99926	1	1	2.7518×10^{-5}

In this way, by standardizing the element size throughout the entire channel, high accuracy in pressure calculations can be achieved. Consequently, this allows for a more precise observation of the effect of the layer arrangement.

Table 3 Mesh independence.

Element size [m]	Number of elements	Number of nodes	Pressure at the third layer outlet [Pa]	Error %
0.001	175	216	764.798	-
0.0005	700	781	764.9881	0.0248
0.00025	2800	2961	765.2008	0.0277
0.0001	17500	17901	763.6494	0.202

Table (3) shows the mesh independence test by showing the increase in the number of elements versus the change in pressure at the outlet of the third layer. This value is pivotal and fundamental for comparing several cases in this study. Since the value of the error was less than 1%, it means that the mesh is independent.

The Grid Convergence Index (GCI) was calculated to assess the effect of mesh size on the results. Richardson's extrapolation method was adopted to estimate the error.

The grid refinement ratio (r) was calculated, and then the order of accuracy (p) was determined using the values of the studied variable. Based on this, the GCI was computed, using equation (6) [23], for both the fine and medium meshes, with the values reaching: $GCI_{fine} = 0.06949686\%$ and $GCI_{medium} = 0.0093946\%$.

$$GCI = \frac{F_s|\emptyset_1 - \emptyset_2|}{\emptyset_1(r_{21}^p - 1)} \times 100\% \quad (6)$$

Where:

$$p = \frac{1}{\ln(r_{21})}\left|\ln\left|\frac{\emptyset_3 - \emptyset_2}{\emptyset_2 - \emptyset_1}\right|\right| \quad (7)$$

The convergence region condition was also verified by comparing the ratio GCI_{fine}/GCI_{medium} with r^p. The results showed good agreement (with a difference of 1.4%), confirming that the numerical solution lies within the convergence region. Accordingly, the adopted mesh satisfies the grid independence condition and is suitable for performing the numerical analysis with high accuracy.

The results of the mesh sensitivity analysis showed that the variation in values between the different meshes was limited, particularly between the medium and fine meshes. The GCI results also supported this conclusion, indicating that the numerical solution is independent of mesh size and that the adopted mesh is suitable for the analysis.

A single mesh was used for the entire channel, with each layer defined as an independent porous zone within the same mesh, where porous layer properties (such as porosity and permeability) were assigned differently for each layer, to represent only the variation in material properties between the regions.

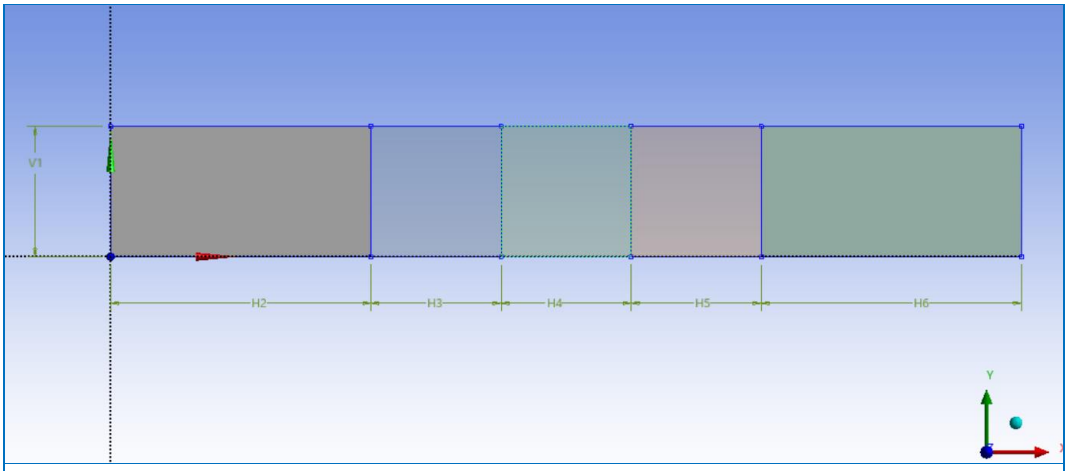


Fig. 1 Sketch design and dimensions in ANSYS Workbench

Figure (1) illustrates the two-dimensional design of the channel with porous layers, where the dimensions of each layer were specified in the ANSYS Workbench software, which were displayed in table (1). It also shows the creation of the surfaces for each layer based on the boundaries of the corresponding sketch.

Table 4 Sketch dimensions.

V1	H2	H3	H4	H5	H6
$5mm$	$10mm$	$5mm$	$5mm$	$5mm$	$10mm$

Table (4) shows the sketch dimensions of the horizontal channel, which contains three porous layers along with the units used. This table helps in reproducing the simulation.

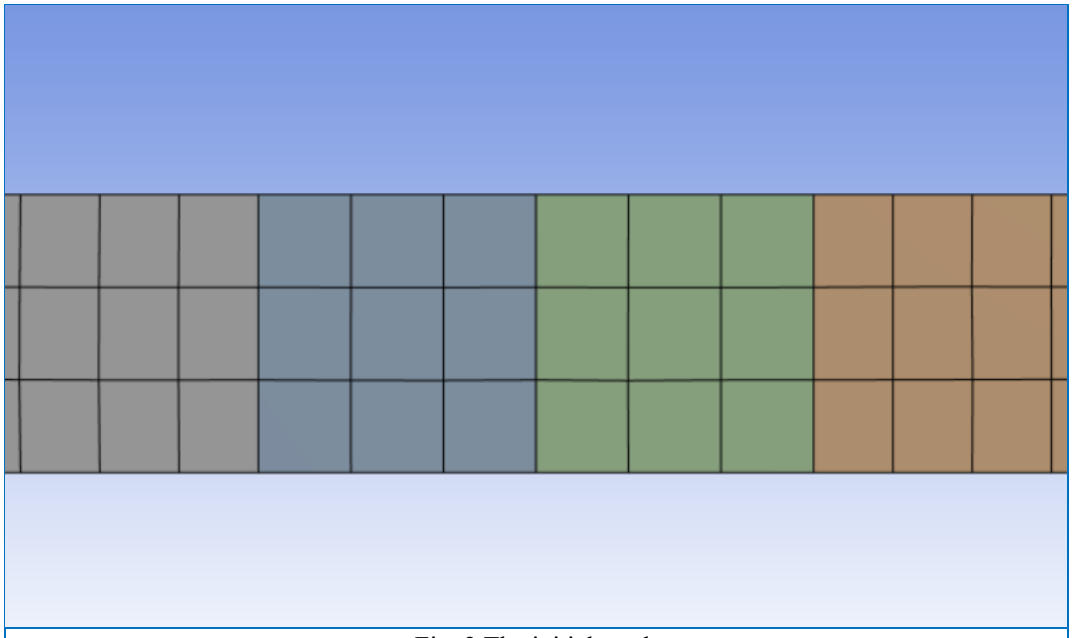


Fig. 2 The initial mesh

Figure (2) illustrates the initial mesh proposed by ANSYS Workbench before making any modifications to the mesh parameters.

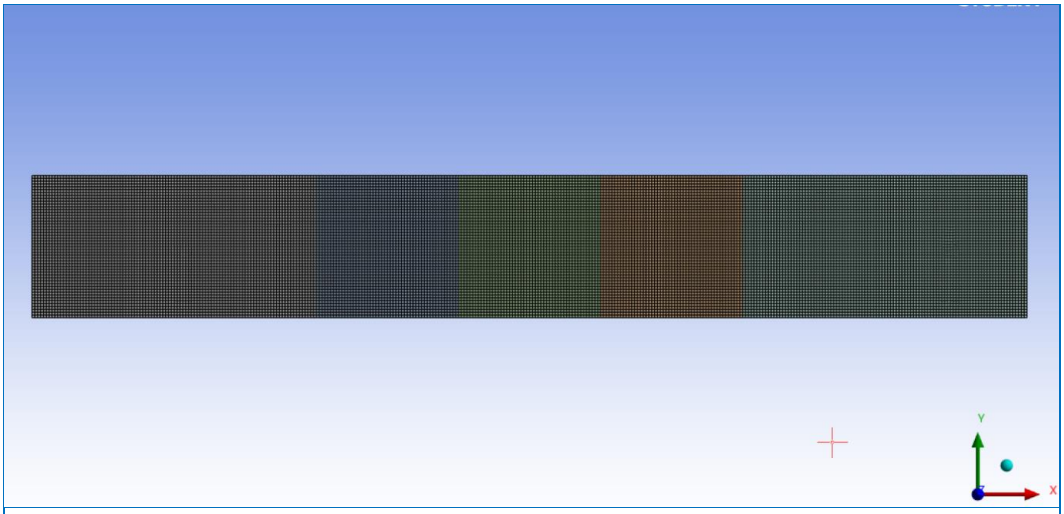


Fig. 3 The modified and adopted mesh in the simulation

Figure (3) shows the final mesh used in the simulation after making the modifications, illustrating the accuracy of its mesh elements. The mesh element size was reduced, resulting in a regular and precise mesh that enables obtaining accurate values.

Details of "Mesh"

Display	
Display Style	Use Geometry Setting
Defaults	
Physics Preference	CFD
Solver Preference	Fluent
Element Size	1.e-004 m
Export Format	Standard
Export Preview Surface Mesh	No
Sizing	
Quality	
Check Mesh Quality	Yes, Errors
Target Skewness	0.2
Smoothing	High
Mesh Metric	None
Inflation	
Advanced	
Automatic Methods	
Sheet Body Method	Quad Dominant
Sweepable Body Method	Sweep
Statistics	

Fig. 4 Basic mesh settings.

Figure (4) shows the basic settings as entered in ANSYS to adjust the mesh resolution.

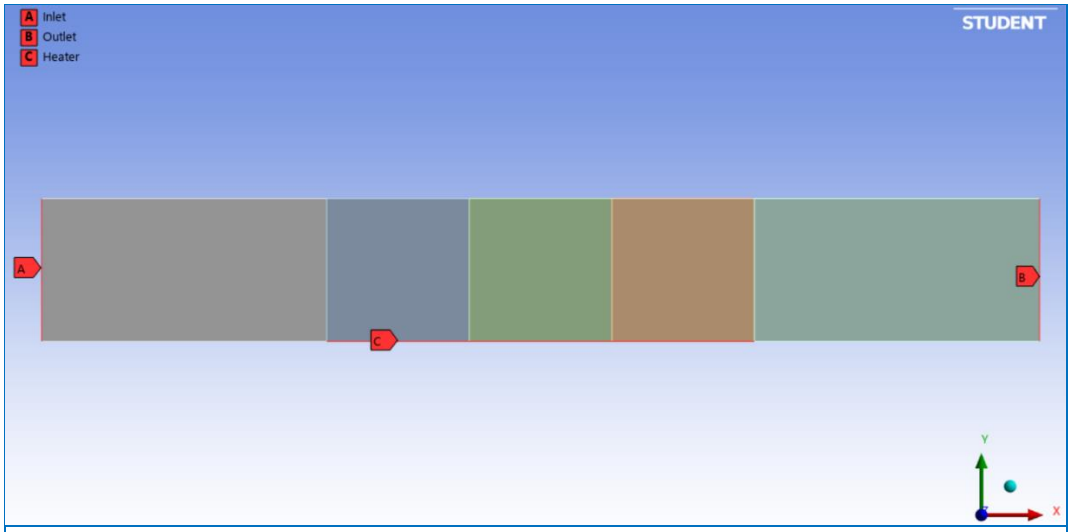


Fig. 5 Boundaries and labels.

Figure (5) shows the identification and naming of the fluid inlet and outlet, as well as identifying and naming the wall heating and the heat exchanger. This figure helps to accurately identify the locations of the functional elements.

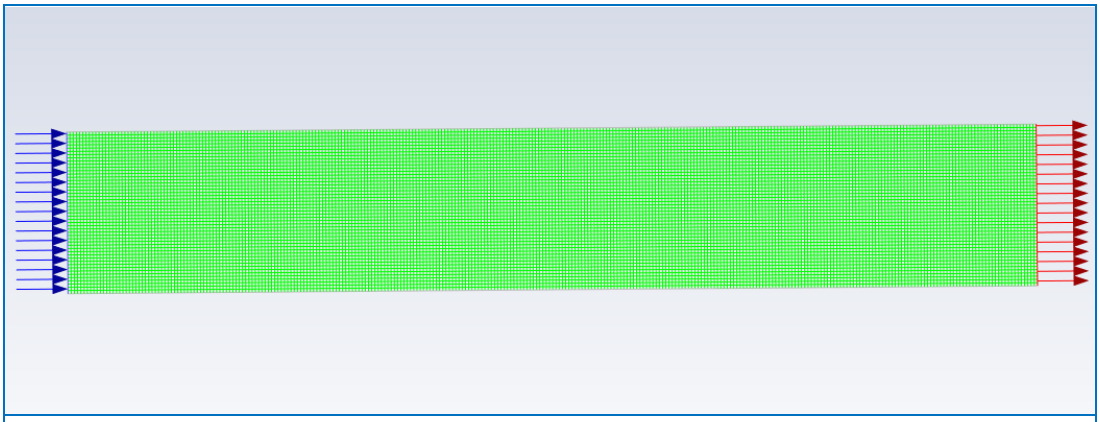


Fig. 6 Setting up the simulation parameters in ANSYS Setup.

Figure (6) illustrates the stage of entering the simulation parameters in ANSYS, where the simulation settings were configured accurately. These parameters are described in table (2). The figure clearly shows the air inlet (arrows colored in blue) and the air outlet on the opposite side (arrows colored in red).

The SIMPLE algorithm was used for pressure-velocity coupling within ANSYS Fluent. Second-order discretization schemes were also employed for the pressure and momentum equations to ensure higher accuracy in the numerical solution. The convergence criteria for the energy and continuity equations were set to 10^{-6}, while a value of 10^{-5} was adopted for the momentum equations, in order to ensure the stability of the numerical solution.

A constant time step of $\Delta t = 1 \times 10^{-4} s$ was employed to ensure numerical stability and temporal accuracy of the solution, selected in accordance with the requirements for capturing the transient flow behavior.

Table 5 The parameters of the simulation.

Inlet velocity $[m/s]$	Outlet pressure [Pa]	Initial air temperature [K]	Heating wall temperature [K]	Reynolds number
3	0	293.15	330	2000

Table (5) illustrates the basic parameters that were input to set up the simulation setting, including the inlet velocity, outlet pressure, initial air temperature, heating wall temperature and Reynolds number to facilitate regenerating the simulation.

Table 6 Properties of air.

$\rho[Kg/m^3]$	$\mu[kg/ms]$	$C_p[J/KgK]$	$k_{cond}[W/mK]$
1.184	1.8×10^{-5}	1005	0.026

Table (6) shows the air properties used in simulating air flow through porous media in a horizontal channel of a heat exchanger in ANSYS, including density, viscosity, specific heat, and thermal conductivity.

Boundary conditions:
1- The left wall was designated as the inlet for the airflow with a constant velocity $v_{in} = 3\,m/s$. At this speed, the flow is laminar and on the border of the transitional flow regime.
It is noted that the classification of flow within the porous medium does not directly depend on the Reynolds number is defined for open-channel flows due to the influence of the porous structure, which enhances viscous damping and limits the development of turbulence. Accordingly, a laminar flow model was adopted, while inertial effects were represented using the Darcy-Forchheimer (Ergun-based formulation) model, eliminating the need to use an explicit turbulence model.
2- The right wall was designated as an air outlet with a fixed pressure $P_{outlet} = 0Pa$.
3- The top and bottom walls represent the channel walls.
4- The heating wall is set at a constant temperature of 330K.
5- A no-slip condition was applied to all boundaries.
6- The initial temperature of the air was set to room temperature, 293.15K, assuming that the fluid is in a homogeneous phase with no initial pressure disturbances.
ANSYS tools were used to record the results, allowing for a clear comparison of the effect of the porous layer arrangement on the pressure distribution.
The numerical model was validated by comparing the simulation results using Computational Fluid Dynamics (CFD) for pressure drop values with those calculated theoretically using the Ergun equation. The comparison showed good agreement between the numerical and theoretical results, which enhances the reliability of the model used and its ability to accurately represent the flow behavior within the porous medium.

Table 7 Pressure drop validation.

$u[m/s]$	ΔP CFD $[Pa]$	ΔP Ergun $[Pa]$
0.5	435.7	420.8
1	848.2	831.9
1.5	1002.15	988.4
2	1193.4	1177.2
2.5	1389.8	1375.2
3	1640.5	1623.4

Table (7) shows the pressure drop values obtained from the numerical simulation results using CFD techniques in ANSYS Fluent at different inlet velocity values. It also presents the pressure drop values calculated from the Ergun equation.
These values were plotted graphically in order to show the extent of agreement between the numerical simulation results and the values calculated from the Ergun equation, and to illustrate the behavior of pressure drop with changes in inlet velocity, which contributes to evaluating the accuracy of the model, and verifying the reliability of its results.

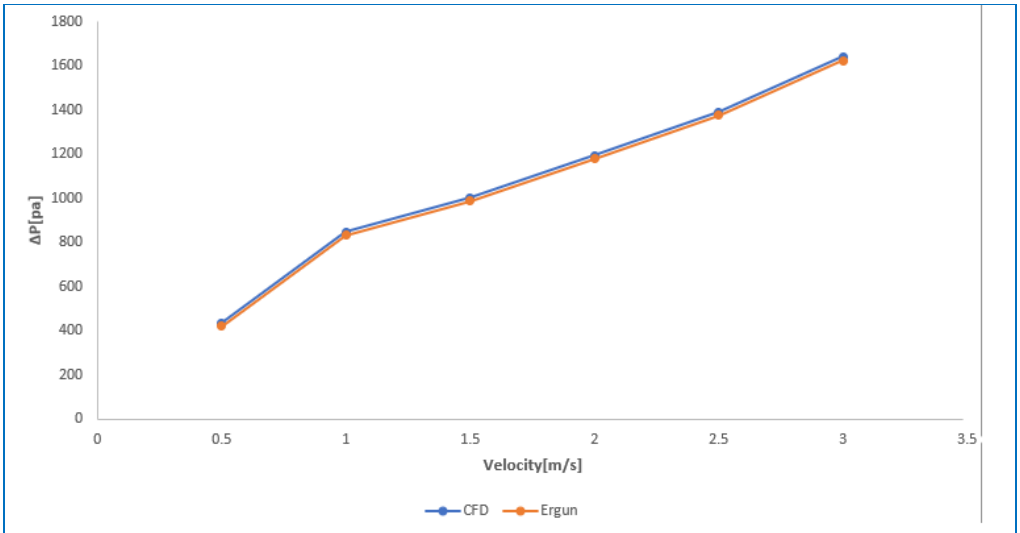


Fig. 7 Validation of pressure drop.

Figure (7) illustrates the relationship between pressure drop and inlet velocity for both numerical simulation results using CFD and the theoretical values calculated from the Ergun equation. It is observed that there is good agreement between the two curves across different inlet velocity values, indicating the accuracy of the numerical model used in representing the flow behavior within the porous medium. The figure also shows an increase in pressure drop with increasing inlet velocity in both cases, which is an expected behavior due to the increase in viscous and inertial resistance forces within the channel. This agreement

confirms the possibility of relying on the numerical model to analyze and predict system performance with high confidence.

4. Simulation results

In this part of the study, the results are reviewed from the CFD simulation and extracted from ANSYS, explaining flow behavior and pressure distribution across porous layers, and the effect of the arrangement of these layers on the pressure drop. The focus of these results was on the effect of the arrangement of the porous layers on the pressure drop and the extent of its effect on the operating efficiency.

Comparison of these results helps to understand the relationship of pressure drop to the arrangement of porous layers, which are a basic and essential factor for reducing pressure losses and thus increasing the heat exchange efficiency in thermal systems and operating efficiency by reducing pressure drop.

Simulation results for six studied cases of porous layer arrangement are presented. Where the distribution of pressure and velocity over the entire channel was presented in general, while the focus was on studying the pressure drop in detail.

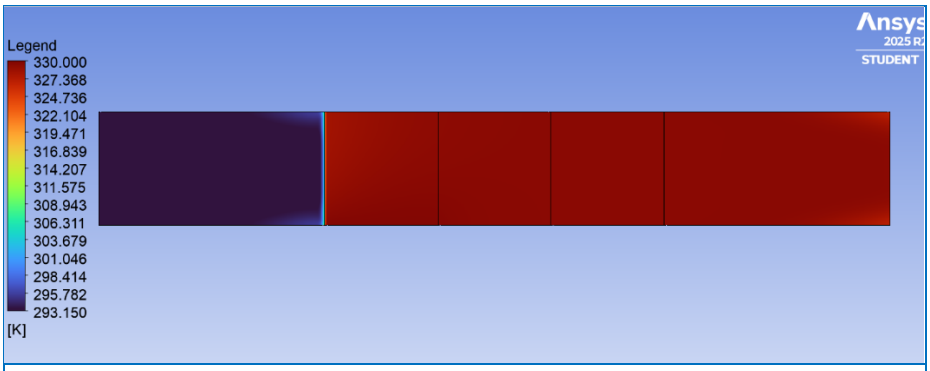


Fig. 8 The Temperature.

Figure (8) shows the temperature distribution along the channel, showing the effectiveness of the porous layers in raising the fluid temperature.

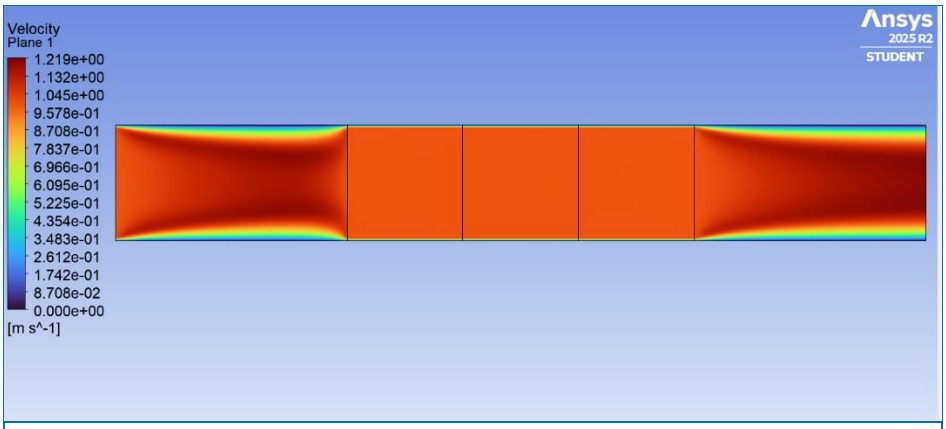
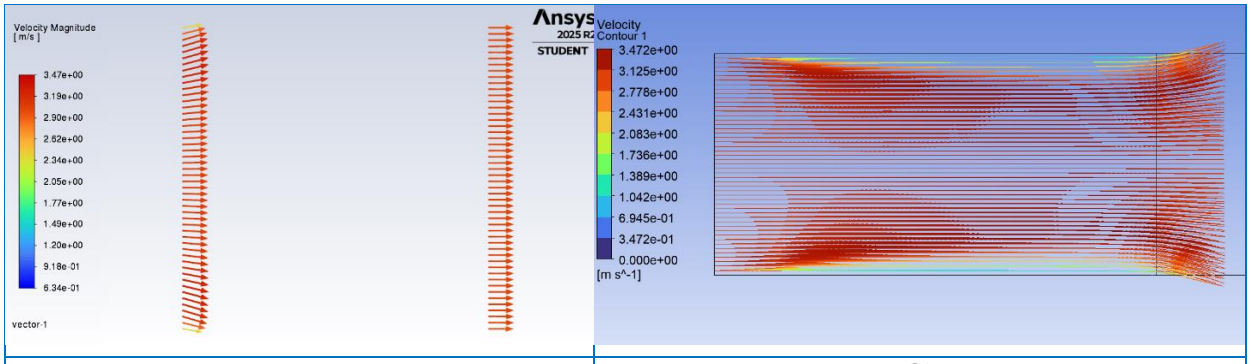


Fig. 9 Velocity distribution.

Figure (9) shows the velocity changes along the channel and in the porous layers, noting the velocity gradient in the areas before and after the porous layers, where it is noted that the velocity is maximum in the center of the channel and decreases towards the side walls of the channel until it becomes zero in the fluid layers in contact with the channel wall [22].

While observed in porous media that the velocity is uniformly distributed, without differences in velocity values within porous media.



(a) (b)

Fig. 10 Velocity vectors.

Figure (10) shows the velocity vectors on the porous layer interface, which illustrates the redistribution of flow upon entering the porous layers, which in turn contributes to the pressure loss.

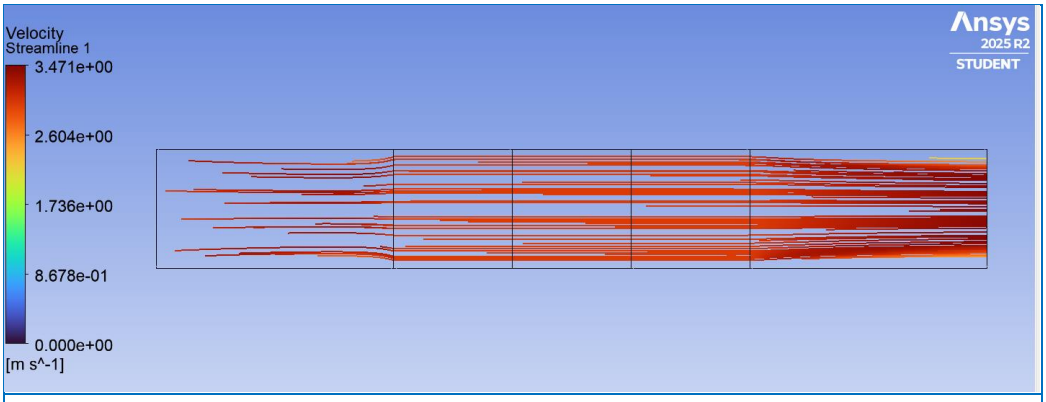


Fig. 11 Velocity streamlines.

Figure (11) shows the streamlines of the velocity along the channel.

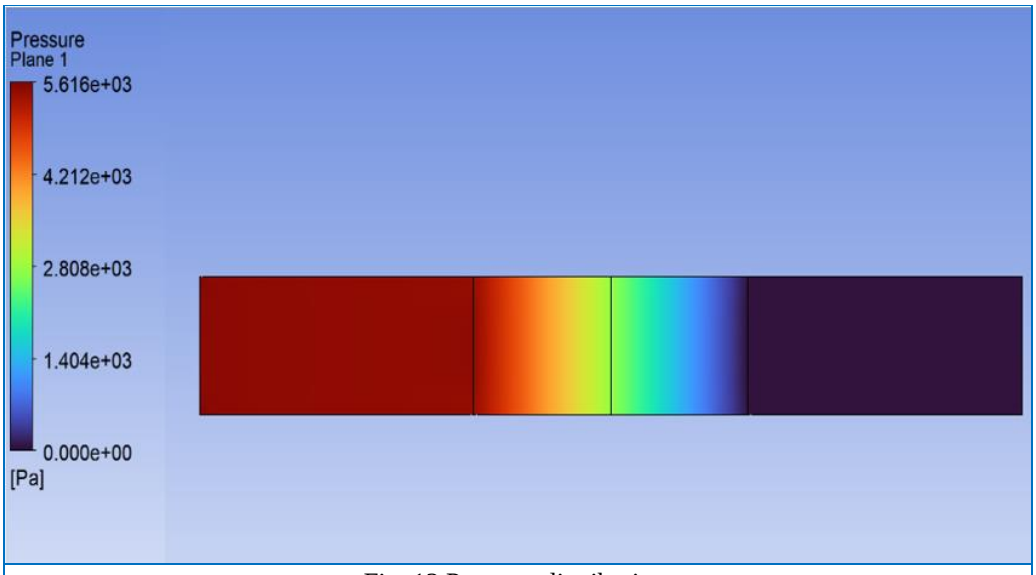


Fig. 12 Pressure distribution.

Figure (12) shows the general pressure distribution and drop along the channel and in the porous layers. As clearly shown by the yellow straight line, which represents the range of points used to draw the plot, the pressure drop along the channel for the different cases.

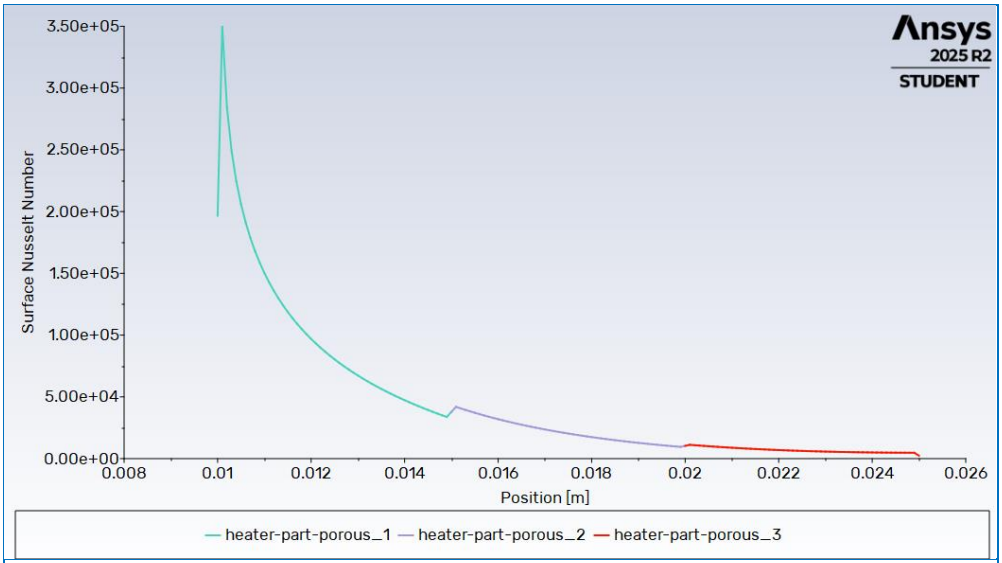


Fig. 13 Nu number.

Figure (13) shows the local Nusselt number for the heated wall in case (5) and its effectiveness in increasing the air temperature within the porous layers.
To verify the effectiveness of the porous layer arrangement on reducing pressure drop without affecting heat transfer, the performance factor was calculated, and its value was 1.34088 according to equation (8).

$$PEC = {(Nu/Nu_0)}\Big/{(f/f_0)^{1/3}} \tag{8}$$

Where:

$$f = \frac{\Delta PD}{0.5\rho u^2 L} \tag{9}$$

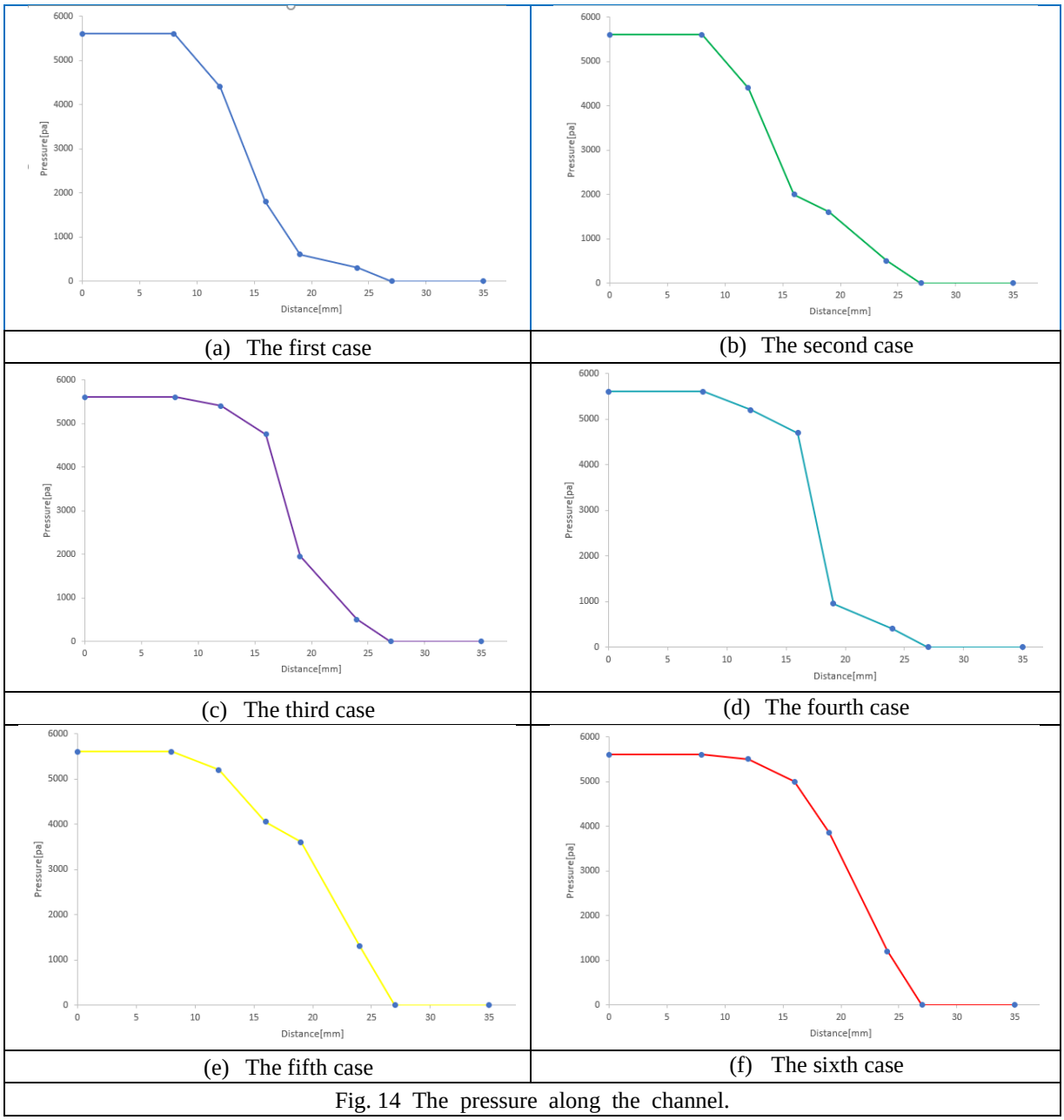
Table 8 The numerical simulation results.

Case no.	Porous layers sequence	Pressure at the first layer inlet [Pa]	Pressure at the third layer outlet [Pa]	Pressure drop [Pa]	Nu [-]
1	0.5-0.6-0.7	3798.574	229.2524	3569.32	174.32
2	0.5-0.7-0.6	3804.201	763.6494	3040.55	181.4
3	0.7-0.5-0.6	5402.238	764.9763	4637.26	162.8
4	0.6-0.5-0.7	4841.696	228.914	4612.78	177.5
5	0.6-0.7-0.5	4853.558	1817.051	3036.5	189.656
6	0.7-0.6-0.5	5386.935	1817.289	3569.646	168.312

Table (8) shows the numerical results of the simulations for the six studied cases of arrangement of porous layers within the cannel. In the first column, the simulation number corresponds to the arrangement

indicated in the second column for the porous layer placement. As shown in this table, the pressure values at the inlet of the first layer and the third layer outlet are presented. The difference in pressure values was also calculated, and then the percentage of pressure reduction between the largest and lowest value was calculated using equation (10), and the obtained value was 34.519%.

$$\Delta = \frac{\Delta P_2 - \Delta P_1}{\Delta P_2} \times 100 \tag{10}$$



(a) The first case (b) The second case

(c) The third case (d) The fourth case

(e) The fifth case (f) The sixth case

Fig. 14 The pressure along the channel.

Figure (14) shows the pressure change along the channel in each of the cases studied. It is noted at first glance that the arrangement of the porous layers affects the pressure, which is through the variation in the shape of the graph line.

The results showed that the pressure distribution along the channel strongly depends on the properties of

each individual layer, where the pressure drop rates vary according to the differences in permeability. In the composite system, the sequential arrangement of layers leads to the formation of an effective permeability that represents the overall system behavior, which is governed by the total resistance resulting from all layers rather than the properties of each layer individually.

5. Analysis of results

It was revealed through careful comparison of the results of numerical simulations extracted from the ANSYS, that changing the arrangement of the porous layers without changing the porosity values or the thickness of the layers is an important factor, and it plays an essential role in reducing pressure losses resulting from friction and losses resulting from sudden and large changes in porosity values.

Cases (3) and (4) exhibited the highest pressure drop values and were close in magnitude, with pressure drops of (4637.26 and 4612.78) pa, respectively. While cases (1) and (6) showed approximately the same pressure drop value of 3569pa, with a pressure drop reduction percentage of 23%.

The lowest pressure drop values were observed in cases (2) and (5), with values of 3040.55pa and 3036.5pa, respectively, and a pressure drop reduction of 34.519%.

The results showed that the fifth case with the arrangement (0.6-0.7-0.5) of the porous layers is the best, where the pressure drop reduction value reached 1600.5pa, with a percentage of 34.519%.

Although the pressure drop values are similar between the two cases, the difference in layer arrangement led to a different pressure distribution within the porous medium. The fifth case showed a more balanced pressure distribution due to the placement of the low-porosity layer at the outlet, which contributes to improving flow uniformity compared to the second case. Therefore, the evaluation does not rely only on the total pressure drop value, but also on the characteristics of the internal flow distribution.

The reduction in pressure loss in the fifth case can be explained by the presence of a high-porosity buffer zone that provides lower resistance to the flow, which reduces the pressure gradient and decreases the overall system resistance. In contrast, the linear gradient leads to a continuous change in hydraulic resistance, which increases the losses compared to the case with the buffer zone.

The percentage reduction in pressure drop between the best and worst cases was also calculated according to equation (10). This percentage was 34.5%, which is higher than the reduction percentage reached by Bahrami and Sharifi, 20% through porous layers along the entire channel. This is another positive aspect of this study, as the porous layers were placed transversely in part of the channel.

Accordingly, the arrangement of the porous layers is an essential factor that cannot be ignored because it affects the overall operating efficiency of the thermal system.

6. Conclusions

The simulation results extracted from ANSYS Fluent showed clearly the effect of the arrangement of porous layers on the distribution and drop pressure.

The most important conclusions derived from the analysis of these results:

1- Changing the arrangement of the porous layers only, without changing the porosity values or the thickness significantly affects the uniformity of pressure distribution.
2- The porous layer arrangement (0.6-0.7-0.5) shows an effect on the development of the thermal boundary layer, where the higher porosity in the middle layer improves the flow and reduces the thermal boundary layer thickness, while the final layer with lower porosity causes an increase in turbulence near the wall, thereby improving the overall thermal mixing.
3- The percentage reduction in pressure losses achieved in this study is 34.5%.
4- To minimize pressure drop in multi-layered systems, the highest porosity layer should be placed in the region of maximum velocity gradient.
5- The simulation can also be repeated to study the effect of the arrangement of the porous layers on the pressure drop using different fluids.
6- It is also possible to search for the best site to place these porous layers within the channel.
7- Although the two-dimensional model was used provides a simplified representation of the flow behavior, the three-dimensional nature of flow within porous media may affect the pressure drop values due to non-uniform velocity distribution and flow redirection near the walls. Accordingly,

it is recommended to adopt three-dimensional models in future studies to improve the accuracy of the results.

Hence, the arrangement of the porous layers is an essential factor in reducing the total resistance and thus reducing the pressure losses. This improves the effectiveness of heat exchangers and increases their operational efficiency.

Nomenclature

ε	Porosity [-]
D	Channel diameter [m]
k	Permeability [-]
μ	Fluid viscosity $[kg/ms]$
ρ	Fluid density $[Kg/m^3]$
u	The volumetric velocity of the fluid $[m/s]$
∇P	Pressure gradient within the porous media [Pa]
d_p	Mean particle diameter [m]
V_1	Channel cross-sectional width [mm]
H_2	Distance from the inlet of the first layer to the channel inlet[mm]
H_3	First porous layer width $[mm]$
H_4	Second porous layer width $[mm]$
H_5	Third porous layer width [mm]
H_6	Distance from the third layer outlet to the channel outlet [mm]
k_{cond}	Thermal conductivity $[W/mK]$
PEC	Performance Evaluation Criterion
Nu	Nusselt number
f	Friction factor
L	Channel length

Subscripts

eff	effective
p	particle
$cond$	Conductivity
in	inlet
0	Reference case

Author Contributions: The author contributed to all parts of the current study.
Funding: This study received no external funding.
Conflicts of Interest: The author declares no conflict of interest.

References

[1] Li. Z., Zhang. S., & Yang. X. (2025), "A comprehensive review of printed circuit heat exchangers: fabrication, thermal-hydraulic performance, and reliability". Energies, 18(23),6200. DOI: http://doi.org/10.3390/en18236200/.

[2] Val. E., John. T., Oparaocha. U., Nakitto. S., Oonyu. R., & Okafor. W. (2024), "Advancement in energy efficiency technologies for thermal systems: A comprehensive review". INOSR APPLIED SCIENCES, 12(1):1-20. DOI: http://doi.org./10.59298/INOSRAS/2024/1.1.1010/

[3] Nield. D.A., & Bejan. A. (2022), "Darcy, Forchheimer, Brinkman and Richards: classical hydro mechanical equations and their significance in the light of the theory of porous media". Archive of Applied Mechanics, 92, 619-639. DOI: http://doi.org/10.1007/s00419-020-01802-3/

[4] Konstantin. O., Sergei. A., Sulpan. K., Tatyana. T., Aleksandr. K., Vladimir. K., & Olga. K. (2023), "Increasing thermal efficiency: methods, case studies, and integration of heat exchangers with renewable energy sources and heat pumps for desalination". Energies, 16(13),4930. DOI: http://doi.org/10.3390/en16134930/

[5] Shamsoddini-lori. A., & Vafai. K. (2025), "Flow and heat transfer in porous media under non-standard asymmetric boundary conditions". Symmetry, 17(12), 2183. DOI: http://doi.org/10.3390/sym17122183/

[6] Ibrahim. A. K. (2025), "Heat transfer and flow behavior in porous media: a review". Anbar Journal of Engineering Sciences, 16(2),66-86. DOI: http://doi.org/10.37649/AJES-25-022/

[7] Liao. Y., Li. X., Zhong. W., & Tao. G. (2016), "Study of pressure drop-flow rate and flow resistance characteristics of heated porous materials under local thermal non-equilibrium conditions". International Journal of Heat and Mass Transfer, 102, 528-543. DOI: http://doi.org/10.1016/j.ijheatmasstransfer.2016.05.101/

[8] Yang. H., Li. Y., Ma. B., & Zhu. H. (2021), "Review and a theoretical approach on pressure drop correlations of flow through open-cell metal foam". Materials, 14(12),3153. DOI: http://doi.org/10.3390/ma14123153/

[9] D'Orazio. A., Karimipour. A., & Ranjbarzadeh. R. (2023). "Lattice Boltzmann modelling of fluid flow through porous media: a comparison between pore-structure and representative elementary volume methods". Energies, 16(14), 5354. DOI: http://doi.org/10.3390/en16145354/

[10] Marcello. L., Salvatore. C., Maria. O., William. M. H., Nicola. B., Wilson. KS. C., & Vincenzo. N. (2014), "Numerical analysis of heat transfer and pressure drop in metal foams for different morphological models". Journal of heat transfer, 136(11), 112601. DOI: http://doi.org/10.1115/1.4028113/

[11] Weiping. W., Jinxing. G., Shuwen. Z., Jian. Y., Xianting. D., & Xuehua. Z. (2014), "Numerical study on hydrodynamic characteristics of plate-fin heat exchanger using porous media approach". Computers & chemical engineering, 61, 30-37. DOI: http://doi.org/10.1016/j.compchemeng.2013.10.010/

[12] Osama. H. H., Gamal. I. S., Sabry. MN., & Hegazi. AA. (2022), "Investigation of heat transfer and pressure drop in a porous media with internal heat generation". Thermal Engineering, 32, 101849. DOI: http://doi.org/10.1016/j.csite.2022.101849/

[13] Marcelina. G., Wojciech. L. (2023), "CFD modeling of pressure drop in double-pipe heat exchanger with turbulators using a porous media model". International Journal of heat & technology, 41 (1). DOI: http://doi.org/10.18280/ijht.410117/

[14] Xiank. L., Yuyuan. Z., Yue. Z., & Mian. W. (2024), "Numerical study on fluid flow behavior and heat transfer performance of porous media manufactured by a space holder method". Materials, 17 (11), 2695. DOI: http://doi.org/10.3390/ma17112695/

[15] Bahrami. H. R., & Sharifi. A. E. (2024), "Application of multi-layered porous media for heat transfer optimization in double pipe heat exchangers using neural network and NSGA II". Scientific Reports, 14, Article 31509. DOI: http://doi.org/10.1038/s41598-024-83176-Y/

[16] K. Mahesh., & B. Jayaraman. (2025), "An experimental and numerical investigation to enhance heat transfer in porous heat exchangers for waste heat recovery system". Thermal Science, 190-190. DOI: http://doi.org/10.2298.TSCI250703190M/

[17] S. A. Ali., & MR. Hameed. (2025), "Computational fluid dynamics analysis for heat transfer enhancement in single horizontal pipe heat exchanger full filled using different types of porous material". Journal of Research and Applications in Mechanical Engineering, 13 (2): JRAME-25. https://ph01.tci-thaijo.org/index.php/jrame/article/view/258256/

[18] Mohamad. A., Mostafa. S., & Talib. D. (2025), "A review on theoretical and computational fluid dynamics modeling of coupled heat and mass transfer in fixed beds of adsorbing porous media". Energies, 18(24), 6418. DOI: http://doi.org/10.3390/en18246418/

[19] A. A. Avramenko., Igor. V. S., M. M. Kovetskaya., & Y. Y. Kovetska. (2020), "Darcy-Brinkman-Forchheimer model for film boiling in porous media". Transport in porous media, 134, 503-536. DOI: http://doi.org/10.1007/s11242-020-01452-7/

[20] Amir. A., Mdi. B. J., & Nadiah. H. A. (2022), "Darcy-Forchheimer relation influence on MHD dissipative third-grade fluid flow and heat transfer in porous medium with joule heating effects: A numerical approach". Processes, 10(5), 906. DOI: https://doi.org/10.3390/pr10050906/

[21] Celebican. C., Tanefo. S., Drust. F., & Reichel. C. (2021), "Permeability and the Ergun equation as a basis for permeability measurements of metallic foams and wire meshes". Transport in porous media, 137, 613-627. DOI: http://doi.org/10.1007/s11242-021-01579-1/

[22] Lauga. E., Brenner. M. P., & Stone. H. A. (2024), "Unveiling the mystery of affective slip". Journal of Fluid Mechanics, 1000, F5. DOI: http://doi.org/10.1017/jfm.2024.839/

[23] Barbaric, M., & Guzovic. Z. (2020), "Investigation of the possibilities to improve hydrodynamic performances of micro-hydrokinetic turbines". Energies, 13(17), 4560. DOI: http://doi.org/10.3390/en13174560/